

Realizing a Universal Quantum Gate Set via Double-Braiding of $SU(2)_k$ Anyon Models

Jiangwei Long¹, Zihui Liu¹, Yizhi Li², Jianxin Zhong³ and Lijun Meng^{1,†}

¹ School of Physics and Optoelectronics, Xiangtan University, Xiangtan 411105, Hunan, People's Republic of China

² School of Physics and Electronic Science, Hunan Institute of Science and Technology, Yueyang 414006, People's Republic of China

³ Center for Quantum Science and Technology, Department of Physics, Shanghai University, Shanghai 200444, People's Republic of China

We systematically investigate the implementation of a universal gate set via double-braiding within $SU(2)_k$ anyon models. The explicit form of the double elementary braiding matrices (DEBM) in these models are derived from the F -matrices and R -symbols obtained via the q -deformed representation theory of $SU(2)$. Using these EBM, standard single-qubit gates are synthesized up to a global phase by a Genetic Algorithm-enhanced Solovay-Kitaev Algorithm (GA-enhanced SKA), achieving the accuracy required for fault-tolerant quantum computation with only 2-level decomposition. For two-qubit entangling gates, Genetic Algorithm (GA) yields braidwords of 30 braiding operations that approximate the local equivalence class [CNOT]. Theoretically, we demonstrate that performing double-braiding in a three-anyon (six-anyon) encoding of single-qubit (two-qubit) is topologically equivalent to a protocol requiring the physical manipulation of only one (three) anyons to execute arbitrary braids. Our numerical results provide strong evidence that double-braiding in $SU(2)_k$ anyons models is capable of universal quantum computation. Moreover, the proposed protocol offers a potential new strategy for significantly reducing the number of non-Abelian anyons that need to be physically manipulated in future braiding-based topological quantum computations (TQC).

1 Introduction

Although quantum computing has demonstrated remarkable advantages over classical computing [1], it faces the challenge of decoherence due to susceptibility to environmental noise. Topological quantum computation (TQC) encodes quantum information in robust ground-state degeneracies, thereby providing inherent global protection against local perturbations and emerging as a highly promising paradigm [2]. TQC relies on quasiparticle excitations known as anyons in two-dimensional systems. The idea of performing TQC with non-Abelian anyons was first proposed by Kitaev [3]. While the experimental detection of non-Abelian anyons remains challenging, encouraging progress has been made in topological superconductors [4] and fractional quantum Hall systems [5] toward realizing such exotic particles.

The $SU(2)_k$ anyon models describe a significant family of topological phases [6]. In particular, the potential for universal quantum computation offered by this series of models (specifically for $k > 3$, $k \neq 4$) has motivated substantial research interest, and their computational universality has been established both theoretically [7] and numerically [8].

[†] Corresponding author. E-mail: ljmeng@xtu.edu.cn

The $SU(2)_2$ model corresponds to Ising anyons, which are believed to exist in fractional quantum Hall systems at filling factor $\nu = 5/2$ [9]. The physical realization of this model is often associated with Majorana fermions, which obey identical fusion and braiding rules. The implementation of quantum gates based on Majorana fermions has been widely studied recently [10-12], and their detection in topological superconductors remains a major experimental pursuit [13] [14]. Although Ising anyons are among the most promising candidates for non-Abelian anyons, braiding alone within this model is insufficient for universal quantum computation [15], as it cannot realize a phase gate without supplemental operations [16]. A modified Ising anyon model, recently proposed within the non-semisimple topological quantum field theory framework, achieves computational universality through braiding by introducing an additional transparent particle, *neglecton* α [17].

The $SU(2)_3$ model describes Fibonacci anyons, which constitute the simplest non-Abelian anyon model capable of universal quantum computation via braiding alone (featuring only the vacuum and the Fibonacci anyon in this model) [18]. These anyons are predicted to exist at filling factor $\nu = 12/5$ in fractional quantum Hall systems [19].

The $SU(2)_4$ model corresponds to metaplectic anyons [20]. While braiding operations alone are not sufficient for universal quantum computation within this model, universality can be achieved when supplemented by fusion and measurement operations [21-23]. This anyon type is theoretically associated with the $\nu = 8/3$ fractional quantum Hall state [24].

In contrast to the $SU(2)_2$ (Ising) and $SU(2)_4$ (metaplectic) models, where standard quantum gates can be implemented directly with only a few braiding operations [15,21], constructing standard gates in $SU(2)_k$ models (with $k > 2$ and $k \neq 4$) requires approximating a target unitary operations with increasingly long sequences of elementary braids [8]. This process corresponds to synthesizing a braidword whose overall action approximates a desired quantum gate (up to a global phase). As the length (the number of braiding operations in a braidword) increases, the number of possible sequences grows exponentially, giving rise to the topological quantum compilation problem [25].

Solutions to this problem have been extensively studied and include algebraic approaches [26], Genetic Algorithms (GA) [27], reinforcement learning [28], and Monte Carlo-enhanced Solovay–Kitaev Algorithms [29], and Genetic Algorithm-enhanced Solovay–Kitaev Algorithms (GA-enhanced SKA) [30]. These methods all operate by searching the exponentially large space of braidwords—sequences of elementary braiding matrices (EBMs) corresponding to physical braid operations—to approximate a target unitary matrix. While these methods were initially developed for compiling single-qubit gates in the Fibonacci ($SU(2)_3$) anyon model, they can be readily generalized to other $SU(2)_k$ models with $k > 4$.

For construction two-qubit entangling gates of the Fibonacci anyon model, initial proposals relied on the unique fusion rules ($\tau \otimes \tau = 1 \oplus \tau$, where τ denotes Fibonacci anyon, and 1 denotes vacuum) of the model to implement the controlled-injection approach [31]. An alternative approach approximates the local equivalence class

[CNOT] gate using the EBMs of the two-qubit encoding [32], this method that also extends to $SU(2)_k$ models with $k > 4$. Furthermore, by leveraging cabling concept from knot theory, specific braid sequences can be selected to achieve low-error entangling gates [33].

While the controlled-injection approach based on three-qubit [34] and even N -qubit constructions [35] have been proposed for Fibonacci anyons, the extension of such multi-qubit gate designs to other $SU(2)_k$ models (with $k > 2$, $k \neq 3$) remains relatively unexplored.

In braiding-based TQC, logical gates are typically realized by sequences of elementary braids involving two anyons at a time. Here, we instead consider the use of double-braiding—the consecutive application of two identical braid operations treated as a single effective unit. It has been theoretically established that double-braiding within $SU(2)_k$ anyon models (for $k > 2$, $k \neq 4$) is dense in $SU(2)$ [36]. A key practical advantage of this approach is the reduction in the number of anyons that must be physically manipulated during a computation.

While previous work has demonstrated that universal quantum computation can be achieved by moving a single anyon via injection braiding, this approach requires the insertion of braidwords equivalent to the identity operation to control the positions of anyons, thereby incurring additional braiding steps [37]. In contrast, double-braiding achieves the same reduction in anyon manipulation without introducing such extra operations.

In this work, we explicitly construct a universal gate set from the double elementary braiding matrices (DEBMs) of $SU(2)_k$ models ($k > 2$, $k \neq 4$). Our numerical results demonstrate the universal quantum computational capability of double-braiding in these models. Furthermore, we establish that realizing an arbitrary single (two) -qubit gate requires the active control of only one (three) anyons, respectively.

The paper is structured as follows: Section 2 introduces the $SU(2)_k$ anyon model, the GA and SKA technique. Section 3 presents the numerical results of our gate compilation via double-braiding of $SU(2)_k$ models ($k = 3, 5, 6, 7$). Section 4 provides a concluding summary. The process of solving DEBMs of $SU(2)_k$ models ($k = 3, 5, 6, 7$) are provided in Appendix A. Appendix B illustrates how topological equivalence within the double-braiding framework minimizes the number of anyons that need to be actively controlled.

2 Theoretical Framerwork and Computational Methods

In $SU(2)_k$ anyon models, distinct anyon types are labeled by topological spins ranging from 0 to $k/2$ in steps of $1/2$. Their fusion rules are governed by the associated k -level theory [38]:

$$j_1 \otimes j_2 = \bigoplus_{j=|j_1-j_2|}^{\min\{j_1+j_2, k-j_1-j_2\}} j, \quad (1)$$

where j_1 and j_2 denote the topological spins of the two anyons to be fused, and j represents the topological spin of the fusion outcome. The fusion can yield multiple possible values of j for non-Abelian anyons. The symbol \otimes denotes the fusion

operation, while \oplus indicates the multiplicity of a possible fusion channel.

One qubit can be encoded using either three or four identical anyons [39], provided their fusion exhibits a twofold degenerate channel. For $SU(2)_k$ models with $k \geq 5$, a suitable encoding is realized with three anyons carrying 1/2-topological spin [8]. In the case of $SU(2)_3$ (Fibonacci anyons), the anyon types are effectively reduced from $\{0, 1/2, 1, 3/2\}$ to $\{0, 1\}$ (see FIG. 2 of Ref. [25]). Consequently, one qubit in the $SU(2)_3$ model is constructed from three anyons with 1-topological spin.

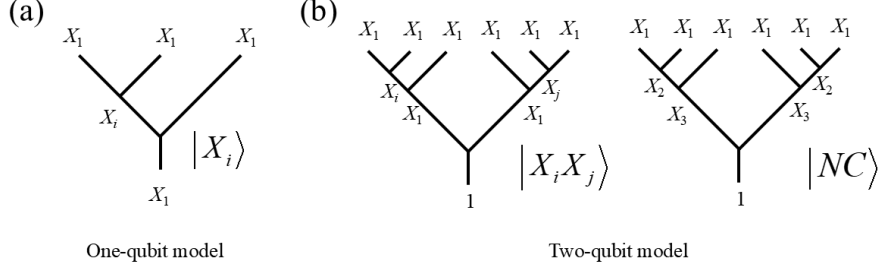


FIG. 1: Schematic of qubit encoding using anyons. (a) A single-qubit is formed by three anyons with 1/2-topological spin. (b) A two-qubit system is composed of six anyons with 1/2-topological spin. Here, the first group of anyons (left) encodes the computational basis states, while the second group (right) resides in a non-computational state.

In the $SU(2)_k$ anyon models ($k \geq 5$), the qubit can be encoded as illustrated in Fig. 1. For clarity, we label distinct anyon types by double their topological spin written as a subscript—e.g., X_1 denotes an anyon with 1/2-topological spin. As shown in Fig. 1(a), three anyons of type X_1 encode a single logical qubit. The fusion of the first and second X_1 yields an intermediate charge, which can be either the vacuum **1** or the anyon X_2 . These two possibilities $\{|1\rangle, |X_2\rangle\}$ correspond to the computational basis states $|0\rangle$ and $|1\rangle$, respectively. The intermediate charge then fuses with the third X_1 to give a final anyon of type X_1 . Fig. 1(b) illustrates the two-qubit encoding using six X_1 anyons. The first and second anyons fuse to an intermediate charge $c_1 \in \{1, X_2\}$, while the fifth and sixth anyons fuse to $c_2 \in \{1, X_2\}$. The four combinations $|c_1, c_2\rangle \in \{|1, 1\rangle, |1, X_2\rangle, |X_2, 1\rangle, |X_2, X_2\rangle\}$ correspond to the two-qubit basis states $\{|0, 0\rangle, |0, 1\rangle, |1, 0\rangle, |1, 1\rangle\}$. These intermediate charges subsequently fuse with the third and fourth X_1 anyons, resulting in two final anyons of type X_1 . Finally, the fusion of these two X_1 anyons yields the overall vacuum charge **1**. Throughout this process, a non-computational state $|NC\rangle$ may also appear.

For the $SU(2)_3$ (Fibonacci) anyon model, the analogous one- and two-qubit encodings are described in Ref. [25] (Fig. 4) and Ref. [40] (Fig. 3), respectively.

Using the encoding scheme shown in Fig. 1(a) with the computational basis $\{|1\rangle, |X_2\rangle\}$ in the $SU(2)_k$ anyon models with ($k \geq 5$), the single-qubit DEBM can be summarized as follows:

$$\left(\sigma_i^{(3)}\right)^2 = \begin{bmatrix} (R_0^{11})^2 & 0 \\ 0 & (R_2^{11})^2 \end{bmatrix}, \quad (2)$$

$$\left(\sigma_2^{(3)}\right)^2 = \begin{bmatrix} F_{1;00}^{111}(R_0^{11})^2(F_{1;00}^{111})^{-1} + F_{1;20}^{111}(R_2^{11})^2(F_{1;20}^{111})^{-1} & F_{1;00}^{111}(R_0^{11})^2(F_{1;02}^{111})^{-1} + F_{1;20}^{111}(R_2^{11})^2(F_{1;22}^{111})^{-1} \\ F_{1;02}^{111}(R_0^{11})^2(F_{1;00}^{111})^{-1} + F_{1;22}^{111}(R_2^{11})^2(F_{1;20}^{111})^{-1} & F_{1;02}^{111}(R_0^{11})^2(F_{1;02}^{111})^{-1} + F_{1;22}^{111}(R_2^{11})^2(F_{1;22}^{111})^{-1} \end{bmatrix}, \quad (3)$$

where R -symbols encode the phase acquired when two identical anyons are exchanged by 180° rotation, while the F -matrices describe the transformation between different fusion bases, with their entries corresponding to specific recoupling coefficients. Their explicit values can be derived from the q -deformed representation theory of $SU(2)$. All necessary F -matrices and R -symbols used in our calculations are provided in the references [8]. The notation $\left(\sigma_i^{(3)}\right)^2$ (with $i = 1, 2$) denotes two successive braiding operations between the i -th and $(i+1)$ -th anyons within the 3-anyon single-qubit encoding.

For the two-qubit encoding in Fig. 1(b), where the basis states are $\{|1, 1\rangle, |1, X_2\rangle, |X_2, 1\rangle, |X_2, X_2\rangle\}$, the corresponding two-qubit DEBM is given by:

$$\left(\sigma_1^{(6)}\right)^2 = (R_2^{11})^2 \oplus \left(\left(\sigma_1^{(3)}\right)^2 \otimes I_2\right), \quad (4)$$

$$\left(\sigma_2^{(6)}\right)^2 = (R_2^{11})^2 \oplus \left(\left(\sigma_2^{(3)}\right)^2 \otimes I_2\right), \quad (5)$$

$$\left(\sigma_4^{(6)}\right)^2 = (R_2^{11})^2 \oplus \left(I_2 \otimes \left(\sigma_2^{(3)}\right)^2\right), \quad (6)$$

$$\left(\sigma_5^{(6)}\right)^2 = (R_2^{11})^2 \oplus \left(I_2 \otimes \left(\sigma_1^{(3)}\right)^2\right), \quad (7)$$

where \oplus denotes the direct sum, \otimes represents the direct product, and I_2 is the 2×2 identity matrix. The notation $\left(\sigma_i^{(3)}\right)^2$ (with $1 \leq i \leq 5$) represents the double braiding of the i -th and $(i+1)$ -th anyons in the 6-anyon two-qubit encoding.

The exact form of the two-qubit operator $\left(\sigma_3^{(6)}\right)^2$ and the detailed derivation procedure are provided in Appendix A.

Apart from deriving DEBMs directly from the F -matrices and R -symbols, they can also be obtained by applying the corresponding EBM twice in succession. Specifically, the DEBMs for the $SU(2)_3$ (Fibonacci) model are constructed by squaring the single-qubit EBMs given in Eqs. (7) and (8) of Ref. [25] and the two-qubit EBMs given in Eqs. (8)–(12) of Ref. [40].

Realizing universal quantum computation via double-braiding of $SU(2)_k$ anyon models (with $k > 2, k \neq 4$) amounts to using the single- and two-qubit DEBMs based on the anyon configurations shown in Fig. 1 to synthesizing a universal gate set [41]:

$$H = \frac{1}{\sqrt{2}} \begin{pmatrix} 1 & 1 \\ 1 & -1 \end{pmatrix}, \quad T = \begin{pmatrix} 1 & 0 \\ 0 & e^{i\pi/4} \end{pmatrix}, \quad \text{CNOT} = \begin{pmatrix} 1 & 0 & 0 & 0 \\ 0 & 1 & 0 & 0 \\ 0 & 0 & 0 & 1 \\ 0 & 0 & 1 & 0 \end{pmatrix}. \quad (8)$$

Standard single-qubit gates such as the Hadamard (H) and phase (T) gates cannot be implemented directly via only a few braiding operations in $SU(2)_k$ anyon models (with $k > 2, k \neq 4$). Consequently, Brute-Force search (BF search) alone is inadequate for constructing high-fidelity single-qubit gates. To address this, we employ the GA-enhanced SKA. The advantage of this approach for compiling high-fidelity single-qubit gates has been demonstrated numerically. Below we outline the method.

The Solovay–Kitaev Algorithm (SKA) allows us to approximate an arbitrary $SU(2)$ unitary matrix (the target high-fidelity H -/ T -gate) to any desired accuracy using a dense set of gates in $SU(2)$ —here, the set of single-qubit DEBMs of the anyon model. In the SKA framework, the 0-level approximation U_0 to the target unitary U is first obtained via a BF search. To reach the 1-level approximation, we should perform the Group Commutator decomposition (GC-decomposition): letting $\Delta = UU_0^\dagger$, then solves $\sin(\theta/2) = 2 \sin^2(\phi/2) \sqrt{1 - \sin^4(\phi/2)}$ to decompose Δ as $VWV^\dagger W^\dagger$. The unitaries V and W are then themselves approximated to 0-level by BF search, yielding V_0 and W_0 . The 1-level approximation to U is then constructed as $U_1 = V_0 W_0 V_0^\dagger W_0^\dagger U_0$.

Higher-level approximations follow recursively by applying the GC-decomposition to V and W . The SKA requires specifying a base braid length l_0 for the 0-level approximation. Each successive increase in the approximation level incurs a factor of 5 increase in the braidword length and a factor of 3 increase in computational time. The details of SKA can be found in Ref. [26].

Although the standard SKA provides a systematic route to high-fidelity single-qubit gates, its clear limitation lies in the BF search for the 0-level approximations. As the l_0 grows, the search space expands exponentially, making BF feasible only for $l_0 \leq 20$. Replacing the BF search with Monte Carlo simulation has been shown to break this length barrier and substantially reduce the time cost. Inspired by this idea, we substitute the BF search with the GA, resulting in a GA-enhanced SKA that delivers improved performance.

The GA mimics natural selection by iteratively evolving a population of candidate solutions (individuals) toward higher fitness [42]. The mapping to topological quantum compilation is natural: a braidword corresponds to an individual; a set of braidwords forms a population; the distance to the target unitary matrix defines the fitness;

mutations alter DEBM within a braidword; and crossover combines segments of two parent braidwords to produce offspring.

3. Numerical Results and Gate Compilation Performance

We employ the GA-enhanced SKA to compile high-fidelity H and T gates from the one-qubit DEBMs of $SU(2)_k$ anyon models ($k = 3, 5, 6, 7$). For two-qubit entangling gates, we use the GA search to approximate braidword belonging to the local equivalence class [CNOT] using the DEBMs of two-qubit. These numerical constructions demonstrate the synthesis of a universal gate set, and we compare the compilation performance achieved with double-braiding against that obtained with single-braiding operations.

In Appendix B, using braidwords obtained from the DEBMs of the $SU(2)_3$ anyon model as examples (specifically, those listed in Table I (single-qubit) and Table II (two-qubit)), we demonstrate how double-braiding enables a topologically equivalent reduction in the number of anyons that need to be actively manipulated.

3.1 Single-Qubit Gate Construction

To quantify the distance between a braidword—constructed from the DEBMs of $SU(2)_k$ anyon models ($k = 3, 5, 6, 7$)—and a target single-qubit gate, we employ the global phase-invariant distance [43]. This metric is insensitive to the overall phase difference, which is physically unobservable in quantum computation, and is defined as:

$$d(U_0, U) = \sqrt{1 - \frac{|\text{Tr}(U_0 U^\dagger)|}{2}}, \quad (9)$$

where U_0 is the matrix representation of the braidword, U^\dagger denotes the conjugate transpose of the target unitary gate U , $\text{Tr}(U_0 U^\dagger)$ denotes the trace of $U_0 U^\dagger$, and $|\text{Tr}(U_0 U^\dagger)|$ denotes the modulus of the $\text{Tr}(U_0 U^\dagger)$.

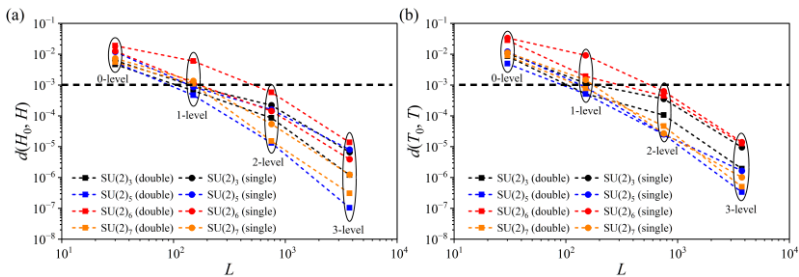


FIG. 2: Construction of standard (a) H -gate and (b) T -gate. The gates are realized via single- and double-braiding in $SU(2)_k$ anyon models ($k = 3, 5, 6, 7$) using the GA-enhanced SKA. Data points achieving the same level of approximation accuracy are grouped by circles. The dashed line indicates the threshold $d = 10^{-3}$.

As shown in Fig. 2, we employ the GA-enhanced SKA to compile standard H and T gates using both EBMs and DEBMs of the $SU(2)_k$ anyon models ($k = 3, 5, 6, 7$). The base length l_0 for the SKA 0-level approximation is set to 30. In the single-braiding scheme (denoted “single”), each elementary operation corresponds to a single braid, and the 0-level braidword thus consists of 30 EBMs. In the double-braiding scheme (denoted “double”), the double braid—i.e., two consecutive identical braids treated as

a single operation—is taken as the basic unit; consequently, the 0-level braidword contains 15 DEBM_s. The 0-level braidwords for the H and T gates obtained via GA search under the double-braiding scheme are summarized in Table I.

Table I. 0-level braidwords and $d(U_0, U)$ metrics for H -/ T -gates. $\{A, B, C, D\}$ corresponding to

$\left\{ \left(\sigma_1^{(3)} \right)^2, \left(\sigma_2^{(3)} \right)^2, \left(\left(\sigma_1^{(3)} \right)^2 \right)^{-1}, \left(\left(\sigma_2^{(3)} \right)^2 \right)^{-1} \right\}$			
	Models	Braidwords	$d(U_0, U)$
H gate	$SU(2)_3$	CDABCDDADCBCBCC	0.00464
	$SU(2)_5$	CBBBADAADABBBC	0.00543
	$SU(2)_6$	BCBBCBADCCBCBAD	0.01887
	$SU(2)_7$	AAABADADADABAAA	0.00550
T gate	$SU(2)_3$	DAABADADADCBADD	0.00860
	$SU(2)_5$	DDAAABBCCBABCCB	0.00491
	$SU(2)_6$	BCCDADCBCBCBCB	0.02826
	$SU(2)_7$	CCDABCDABADADAB	0.00902

For each model and each single-qubit gate, increasing the approximation level of the GA-enhanced SKA leads to a systematic decrease in the $d(U_0, U)$. According to the threshold theorem [44,45], a gate error below 1% ($d(U_0, U) < 10^{-2}$) is sufficient for fault-tolerant quantum computation. We adopt a more stringent criterion, demanding $d(U_0, U) < 10^{-3}$ (the region below the black dashed line in Fig. 2). This requirement is already satisfied at the 2-level approximation for both gates, with typical distances in the range $10^{-5} < d(H_0, H), d(T_0, T) < 10^{-3}$. If even higher accuracy is desired, the 3-level approximation can be reached, yielding distances $10^{-8} < d(H_0, H) < 10^{-4}$ and $10^{-7} < d(T_0, T) < 10^{-4}$.

Remarkably, for all models under investigation, double-braiding consistently outperforms single-braiding in compiling the H and T gates: the distances $d(H_0, H)$ and $d(T_0, T)$ obtained from DEBM_s are almost universally lower than those obtained from EBM_s. The only exception is the H gate compiled with the $SU(2)_6$ model, where single-braiding yields a slightly better approximation.

3.2 Two-Qubit Entangling Gate and Leakage Error Analysis

Makhlin first proposed characterizing two-qubit gates by three real parameters—the so-called local invariants—which uniquely determine the local equivalence class of a given gate [46]. Subsequently, Zhang et al. developed a geometric theory of two-qubit operations by combining these invariants with the Cartan decomposition of the Lie group $SU(4)$ [47]. Two different two-qubit gates belong to the same local equivalence class they can be interconverted by some single-qubit operations. It has been shown that approximating the local equivalence class of a target two-qubit gate is significantly more efficient than approximating the gate itself [48].

Burke et al. demonstrated that high-fidelity approximations to the local equivalence class [CNOT] can be achieved using braidwords constructed from two-qubit EBM_s in the $SU(2)_3$ (Fibonacci) anyon model [32]. Subsequent work has shown that EBM_s of $SU(2)_k$ models (with $k = 5, 6, 7$) also enable high-precision

approximations to [CNOT] [8].

In the present work, we construct braidwords B using DEBM s of $SU(2)_k$ anyon models ($k = 3, 5, 6, 7$). Each such braidword acts on a five-dimensional Hilbert space, which decomposes as a direct sum of a one-dimensional non-computational subspace and a four-dimensional computational subspace. Correspondingly, the matrix representation of B takes the block-diagonal form $B = M \oplus A$, where M is a complex number acting on the non-computational sector and A is a 4×4 matrix acting on the computational sector. The procedure for extracting the local equivalence class of a given braidword and comparing it to that of the CNOT gate is detailed in Ref. [32].

The distance between the braidword and the local equivalence class [CNOT] is defined:

$$d^{\text{CNOT}}(A) = \sum_{i=1}^3 \Delta g_i^2, \Delta g_i = |g_i(A) - g_i(\text{CNOT})|, \quad (10)$$

where $g_i(A)$ denotes the i -th local invariant of A , and $g_1(\text{CNOT}) = 0, g_2(\text{CNOT}) = 0, g_3(\text{CNOT}) = 1$. Leakage errors (arising from the eight off-block-diagonal elements of B that couple the computational and non-computational subspaces) must be suppressed to prevent population loss from the computational space. To this end,

$M_{11} = \sqrt{M^* M} \approx 1$ is required [40]; we enforce $M_{11} > 0.99$ in the numerical calculations.

Furthermore, to ensure that A is sufficiently close to unitary, unitary measurement is defined:

$$d^U = \text{Tr}(\sqrt{a^\dagger a}), \quad (11)$$

where $a = A^\dagger A - I$, and I is a four-dimensional identity matrix. The condition $d^U < 0.1$ is imposed to ensure the unitarity of computational matrix A .

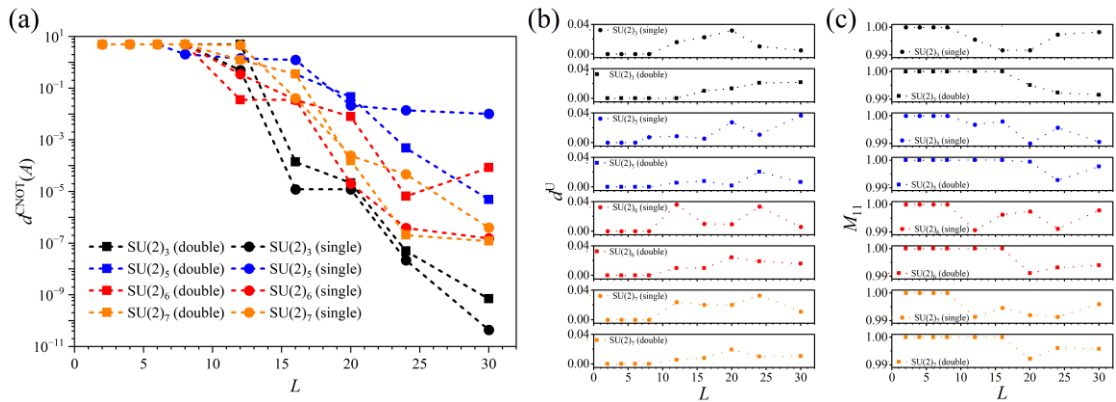


FIG. 3: Approximation of the local equivalence class [CNOT] via braiding. (a) Results compiled using single- and double-braiding in $SU(2)_k$ anyon models ($k = 3, 5, 6, 7$). Searches are constrained by (b) the unitary measurement of A $d^U < 0.1$, and (c) the $|M_{11}| > 0.99$. The data were obtained as follows: for single-braiding, by BF search ($L = 2, 4, 6, 8$) and by GA ($L = 12, 16, 20, 24, 30$); for double-braiding, by BF search ($L = 2, 4, 6, 8, 12, 16$) and by GA ($L = 20, 24, 30$).

The results of approximating the local equivalence class [CNOT] using

braidwords constructed from both single-braiding (EBM) and double-braiding (DEBM) operations in $SU(2)_k$ anyon models ($k = 3, 5, 6, 7$) as shown in Fig. 3. The braidwords are obtained via BF search or GA, subject to the constraints $d^U < 0.1$ and $M_{11} > 0.99$.

The computational results demonstrate that increasing the braid length L via GA systematically reduces the $d^{\text{CNOT}}(A)$ to the target local equivalence class. Notably, for $L = 30$, the $SU(2)_3$ model exhibits a significant advantage in approximating the local equivalence class [CNOT], achieving distances in the range $10^{-11} < d^{\text{CNOT}}(A) < 10^{-9}$. For the $SU(2)_{5,6,7}$ models, the achieved distances lie within $10^{-7} < d^{\text{CNOT}}(A) < 10^{-4}$, with the exception of single-braiding in the $SU(2)_6$ model, where $d^{\text{CNOT}}(A)$ remains around 10^{-2} . However, employing double-braiding for the $SU(2)_6$ model reduces $d^{\text{CNOT}}(A)$ to approximately 10^{-5} .

For $L = 30$, detailed results (including the explicit braidwords, $d^{\text{CNOT}}(A)$, d^U , and M_{11}) obtained using DEBMs to approximate the local equivalence class [CNOT] for all $SU(2)_k$ models ($k = 3, 5, 6, 7$) are summarized in Table II. These numerical findings confirm that double-braiding in $SU(2)_k$ anyon models ($k = 3, 5, 6, 7$) provides an effective means of realizing high-fidelity two-qubit entangling gates.

Table II. Braidwords yielding the $d^{\text{CNOT}}(A)$, d^U , and M_{11} for the CNOT-gates were obtained via

GA. $\{A, B, C, D, E, F, G, H, I, J\}$ corresponding to

$$\left\{ \left(\sigma_1^{(6)} \right)^2, \left(\sigma_2^{(6)} \right)^2, \left(\sigma_3^{(6)} \right)^2, \left(\sigma_4^{(6)} \right)^2, \left(\sigma_5^{(6)} \right)^2, \left(\left(\sigma_1^{(6)} \right)^2 \right)^{-1}, \left(\left(\sigma_2^{(6)} \right)^2 \right)^{-1}, \left(\left(\sigma_3^{(6)} \right)^2 \right)^{-1}, \left(\left(\sigma_4^{(6)} \right)^2 \right)^{-1}, \left(\left(\sigma_5^{(6)} \right)^2 \right)^{-1} \right\}.$$

	Models	Braidwords	$d^{\text{CNOT}}(A)$	d^U	M_{11}
CNOT-gate	$SU(2)_3$	HGEHGFBAEABFGGC	7.00953×10^{-10}	0.02171	0.99158
	$SU(2)_5$	CDJAHDDAJJHHFIC	4.89496×10^{-6}	0.00646	0.99767
	$SU(2)_6$	GGCGGFFGJAHBCC	8.48726×10^{-5}	0.01588	0.99397
	$SU(2)_7$	HBCIBBBADGGAHBC	1.21880×10^{-7}	0.01053	0.99580

4 Conclusion and Future Prospects

In this work, we explicitly construct a high-fidelity universal quantum gate set $\{H, T, \text{CNOT}\}$ via numerical simulation using the DEBMs of $SU(2)_k$ anyon models ($k = 3, 5, 6, 7$). Specifically, employing the GA-enhanced SKA, we achieve fault-tolerant precision for the H and T gates at only the 2-level approximation (with the base length $l_0 = 30$). For the two-qubit CNOT gate, the GA search extending the braid length to $L = 30$ yields an approximation to its local equivalence class with distance $d^{\text{CNOT}}(A) < 10^{-4}$. These results provide crucial numerical evidence supporting the universality of double-braiding in $SU(2)_k$ anyon models ($k \geq 3, k \neq 4$).

Furthermore, double-braiding enables the topologically equivalent reduction in the number of non-Abelian anyons that require active manipulation. Concretely, single-qubit operations can be implemented by moving only one anyon, and two-qubit operations by moving only three anyons. This feature significantly alleviates the practical difficulty of manipulating anyons in future TQC platforms based on topological superconductors or fractional quantum Hall systems.

Funding This work is supported by the National Natural Science Foundation of China (Grant Nos. 12374046, 11204261), College of Physics and Optoelectronic Engineering training program, a Key Project of the Education Department of Hunan Province (Grant No. 19A471), Natural Science Foundation of Hunan Province (Grant No. 2018JJ2381), Shanghai Science and Technology Innovation Action Plan (Grant No. 24LZ1400800), Education Department of Hunan Province (Grant No. 24C0316).

Data Availability Statement The datasets generated during and/or analyzed during the current study are available from the corresponding author on reasonable request

Declarations

Conflict of interest No potential conflict of interest was reported by the authors. All authors of this manuscript have read and approved the final version submitted, and contents of this manuscript have not been copyrighted or published previously and are not under consideration for publication elsewhere.

Appendix A: Derivation of the Exact DEBM

We present a general procedure for constructing the DEBM in $SU(2)_k$ anyon models within the anyon configuration illustrated in Fig. 1.

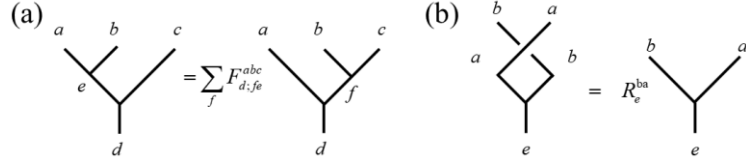


FIG. 4: The definitions of (a) the F -move (fusion) and (b) the R -move (rotation).

The braiding operations are implemented via F -moves (transformations between distinct fusion bases) and R -moves (rotations), as defined in Fig. 4.

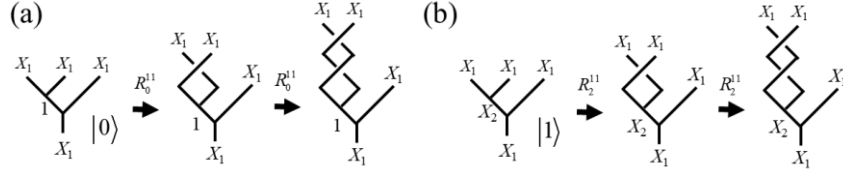


FIG. 5: The operator $(\sigma_1^{(3)})^2$ acting on (a) $|0\rangle$ and (b) $|1\rangle$ in the single-qubit configuration.

For a single qubit encoded in three anyons, applying two consecutive R operations to the computational basis states $|0\rangle$ and $|1\rangle$ ($|0\rangle = [1 \ 0]^T, |1\rangle = [0 \ 1]^T$.) for braiding the anyons of first two as shown in Fig. 5 yields:

$$(\sigma_1^{(3)})^2 |0\rangle = (R_0^{11})^2 |0\rangle, \quad (12)$$

$$(\sigma_1^{(3)})^2 |1\rangle = (R_2^{11})^2 |1\rangle, \quad (13)$$

Eqs. (12) and (13) can be combined to yield Eq. (2).

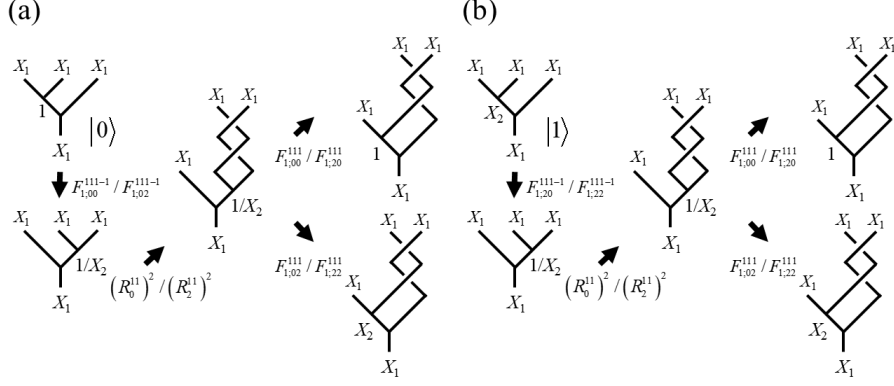


FIG. 6: The operator $(\sigma_2^{(3)})^2$ acting on (a) $|0\rangle$ and (b) $|1\rangle$ in the single-qubit configuration.

To braid the latter two anyons, one first applies an F -move to transform from the fusion basis of the first two anyons to last two, then performs two consecutive R -moves, and finally applies an inverse F -move to return to the original fusion basis. This sequence, illustrated in Fig. 6, yields the following results when acting on $|0\rangle$ and $|1\rangle$, respectively:

$$(\sigma_2^{(3)})^2 |0\rangle = \left(F_{1,00}^{111} (R_0^{11})^2 (F_{1,00}^{111})^{-1} + F_{1,20}^{111} (R_2^{11})^2 (F_{1,02}^{111})^{-1} \right) |0\rangle + \left(F_{1,02}^{111} (R_0^{11})^2 (F_{1,00}^{111})^{-1} + F_{1,22}^{111} (R_2^{11})^2 (F_{1,02}^{111})^{-1} \right) |1\rangle, \quad (14)$$

$$(\sigma_2^{(3)})^2 |1\rangle = \left(F_{1,00}^{111} (R_0^{11})^2 (F_{1,20}^{111})^{-1} + F_{1,20}^{111} (R_2^{11})^2 (F_{1,22}^{111})^{-1} \right) |0\rangle + \left(F_{1,02}^{111} (R_0^{11})^2 (F_{1,20}^{111})^{-1} + F_{1,22}^{111} (R_2^{11})^2 (F_{1,22}^{111})^{-1} \right) |1\rangle, \quad (15)$$

Eqs. (14) and (15) can be combined to yield Eq. (3).

For the two-qubit system encoded in the six-anyon configuration shown in Fig. 1, performing local braiding on the first and second anyons (corresponding to $(\sigma_1^{(6)})^2$)

and on the fifth and sixth anyons (corresponding to $(\sigma_5^{(6)})^2$) by applying two consecutive R -moves to each of the basis states ($|NC\rangle = [1 \ 0 \ 0 \ 0 \ 0]^T$,

$$|00\rangle = [0 \ 1 \ 0 \ 0 \ 0]^T, \quad |01\rangle = [0 \ 0 \ 1 \ 0 \ 0]^T, \quad |10\rangle = [0 \ 0 \ 0 \ 1 \ 0]^T,$$

$$|11\rangle = [0 \ 0 \ 0 \ 0 \ 1]^T$$

yields:

$$(\sigma_1^{(6)})^2 |NC\rangle = (R_2^{11})^2 |NC\rangle, \quad (16)$$

$$(\sigma_1^{(6)})^2 |00\rangle = (R_0^{11})^2 |00\rangle, \quad (17)$$

$$(\sigma_1^{(6)})^2 |01\rangle = (R_0^{11})^2 |01\rangle, \quad (18)$$

$$(\sigma_1^{(6)})^2 |10\rangle = (R_2^{11})^2 |10\rangle, \quad (19)$$

$$(\sigma_1^{(6)})^2 |11\rangle = (R_2^{11})^2 |11\rangle, \quad (20)$$

$$\left(\sigma_5^{(6)}\right)^2 |NC\rangle = \left(R_2^{11}\right)^2 |NC\rangle, \quad (21)$$

$$\left(\sigma_5^{(6)}\right)^2 |00\rangle = \left(R_0^{11}\right)^2 |00\rangle, \quad (22)$$

$$\left(\sigma_5^{(6)}\right)^2 |01\rangle = \left(R_2^{11}\right)^2 |01\rangle, \quad (23)$$

$$\left(\sigma_5^{(6)}\right)^2 |10\rangle = \left(R_0^{11}\right)^2 |10\rangle, \quad (24)$$

$$\left(\sigma_5^{(6)}\right)^2 |11\rangle = \left(R_2^{11}\right)^2 |11\rangle, \quad (25)$$

Eqs. (16)~(20) can be combined to yield Eq. (4), and Eqs. (21)~(25) can be combined to yield Eq. (7).

For the two-qubit system, performing local braiding on the second and third anyons (corresponding to $\left(\sigma_2^{(6)}\right)^2$) and on the fourth and fifth anyons (corresponding to $\left(\sigma_4^{(6)}\right)^2$), analogous to the action of $\left(\sigma_2^{(3)}\right)^2$ in the three-anyon single-qubit encoding, requires first applying an F -move to transform to the appropriate fusion basis, then performing two consecutive R -moves, and finally applying the F -move to return to the original basis. Acting on the basis states $|NC\rangle, |00\rangle, |01\rangle, |10\rangle, |11\rangle$, this sequence yields:

$$\left(\sigma_2^{(6)}\right)^2 |NC\rangle = \left(R_2^{11}\right)^2 |NC\rangle, \quad (26)$$

$$\left(\sigma_2^{(6)}\right)^2 |00\rangle = \left(F_{1;00}^{111}\left(R_0^{11}\right)^2 \left(F_{1;00}^{111}\right)^{-1} + F_{1;20}^{111}\left(R_2^{11}\right)^2 \left(F_{1;20}^{111}\right)^{-1}\right) |00\rangle + \left(F_{1;02}^{111}\left(R_0^{11}\right)^2 \left(F_{1;00}^{111}\right)^{-1} + F_{1;22}^{111}\left(R_2^{11}\right)^2 \left(F_{1;20}^{111}\right)^{-1}\right) |10\rangle, \quad (27)$$

$$\left(\sigma_2^{(6)}\right)^2 |01\rangle = \left(F_{1;00}^{111}\left(R_0^{11}\right)^2 \left(F_{1;00}^{111}\right)^{-1} + F_{1;20}^{111}\left(R_2^{11}\right)^2 \left(F_{1;20}^{111}\right)^{-1}\right) |01\rangle + \left(F_{1;02}^{111}\left(R_0^{11}\right)^2 \left(F_{1;00}^{111}\right)^{-1} + F_{1;22}^{111}\left(R_2^{11}\right)^2 \left(F_{1;20}^{111}\right)^{-1}\right) |11\rangle, \quad (28)$$

$$\left(\sigma_2^{(6)}\right)^2 |10\rangle = \left(F_{1;00}^{111}\left(R_0^{11}\right)^2 \left(F_{1;02}^{111}\right)^{-1} + F_{1;20}^{111}\left(R_2^{11}\right)^2 \left(F_{1;22}^{111}\right)^{-1}\right) |00\rangle + \left(F_{1;02}^{111}\left(R_0^{11}\right)^2 \left(F_{1;02}^{111}\right)^{-1} + F_{1;22}^{111}\left(R_2^{11}\right)^2 \left(F_{1;22}^{111}\right)^{-1}\right) |10\rangle, \quad (29)$$

$$\left(\sigma_2^{(6)}\right)^2 |11\rangle = \left(F_{1;02}^{111}\left(R_0^{11}\right)^2 \left(F_{1;02}^{111}\right)^{-1} + F_{1;22}^{111}\left(R_2^{11}\right)^2 \left(F_{1;22}^{111}\right)^{-1}\right) |01\rangle + \left(F_{1;02}^{111}\left(R_0^{11}\right)^2 \left(F_{1;02}^{111}\right)^{-1} + F_{1;22}^{111}\left(R_2^{11}\right)^2 \left(F_{1;22}^{111}\right)^{-1}\right) |11\rangle, \quad (30)$$

$$\left(\sigma_4^{(6)}\right)^2 |NC\rangle = \left(R_2^{11}\right)^2 |NC\rangle, \quad (31)$$

$$\left(\sigma_4^{(6)}\right)^2 |00\rangle = \left(F_{1;00}^{111}\left(R_0^{11}\right)^2 \left(F_{1;00}^{111}\right)^{-1} + F_{1;20}^{111}\left(R_2^{11}\right)^2 \left(F_{1;20}^{111}\right)^{-1}\right) |00\rangle + \left(F_{1;02}^{111}\left(R_0^{11}\right)^2 \left(F_{1;00}^{111}\right)^{-1} + F_{1;22}^{111}\left(R_2^{11}\right)^2 \left(F_{1;20}^{111}\right)^{-1}\right) |01\rangle, \quad (32)$$

$$\left(\sigma_4^{(6)}\right)^2 |01\rangle = \left(F_{1;00}^{111}\left(R_0^{11}\right)^2 \left(F_{1;02}^{111}\right)^{-1} + F_{1;20}^{111}\left(R_2^{11}\right)^2 \left(F_{1;22}^{111}\right)^{-1}\right) |00\rangle + \left(F_{1;02}^{111}\left(R_0^{11}\right)^2 \left(F_{1;02}^{111}\right)^{-1} + F_{1;22}^{111}\left(R_2^{11}\right)^2 \left(F_{1;22}^{111}\right)^{-1}\right) |01\rangle, \quad (33)$$

$$\left(\sigma_4^{(6)}\right)^2 |10\rangle = \left(F_{1;00}^{111}\left(R_0^{11}\right)^2 \left(F_{1;00}^{111}\right)^{-1} + F_{1;20}^{111}\left(R_2^{11}\right)^2 \left(F_{1;20}^{111}\right)^{-1}\right) |01\rangle + \left(F_{1;02}^{111}\left(R_0^{11}\right)^2 \left(F_{1;00}^{111}\right)^{-1} + F_{1;22}^{111}\left(R_2^{11}\right)^2 \left(F_{1;20}^{111}\right)^{-1}\right) |11\rangle, \quad (34)$$

$$\left(\sigma_4^{(6)}\right)^2 |11\rangle = \left(F_{1;00}^{111}\left(R_0^{11}\right)^2 \left(F_{1;02}^{111}\right)^{-1} + F_{1;20}^{111}\left(R_2^{11}\right)^2 \left(F_{1;22}^{111}\right)^{-1}\right) |01\rangle + \left(F_{1;02}^{111}\left(R_0^{11}\right)^2 \left(F_{1;02}^{111}\right)^{-1} + F_{1;22}^{111}\left(R_2^{11}\right)^2 \left(F_{1;22}^{111}\right)^{-1}\right) |11\rangle, \quad (35)$$

Eqs. (26)~(30) can be combined to yield Eq. (5), and Eqs. (31)~(35) can be combined

to yield Eq. (6).

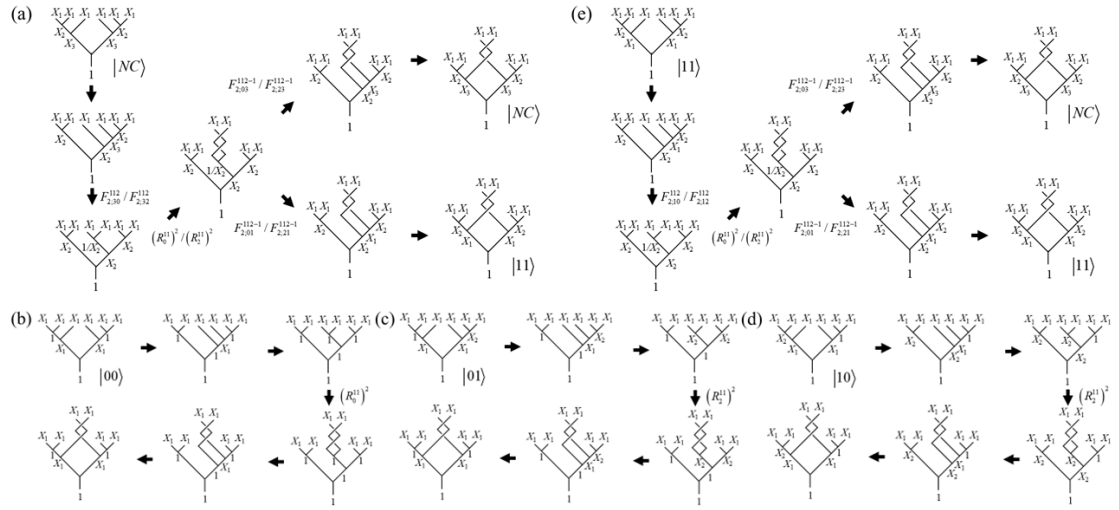


FIG. 7: The operator $(\sigma_3^{(6)})^2$ acting on (a) $|NC\rangle$, (b) $|00\rangle$, (c) $|01\rangle$, (d) $|10\rangle$, (e) $|11\rangle$ in the two-qubit configuration.

As illustrated in Fig. 7, performing braiding operations on the third and fourth anyons within the two-qubit basis by applying F - and R -moves (Note that trivial F -moves are omitted in fig. 7 for simplicity), yields:

$$\left(\sigma_3^{(6)}\right)^2 |NC\rangle = \left(F_{2,03}^{112} \left(R_0^{11}\right)^2 \left(F_{2;30}^{112}\right)^{-1} + F_{2;23}^{112-1} \left(R_2^{11}\right)^2 \left(F_{2;32}^{112}\right)^{-1}\right) |NC\rangle + \left(F_{2;01}^{112-1} \left(R_0^{11}\right)^2 \left(F_{2;30}^{112}\right)^{-1} + F_{2;21}^{112-1} \left(R_2^{11}\right)^2 \left(F_{2;32}^{112}\right)^{-1}\right) |11\rangle \quad (36)$$

$$\sigma_3^{(6)}|00\rangle = \left(R_0^{11}\right)^2 |00\rangle \quad (37)$$

$$\sigma_3^{(6)}|01\rangle = (R_2^{11})^2 |01\rangle \quad (38)$$

$$\sigma_3^{(6)}|10\rangle = \left(R_2^{11}\right)^2 |10\rangle \quad (39)$$

$$\left(\sigma_3^{(6)}\right)^2 |11\rangle = \left(F_{2;03}^{112-1} \left(R_0^{11}\right)^2 F_{2;10}^{112} + F_{2;23}^{112-1} \left(R_2^{11}\right)^2 F_{2;12}^{112}\right) |NC\rangle + \left(F_{2;01}^{112-1} \left(R_0^{11}\right)^2 F_{2;10}^{112} + F_{2;21}^{112-1} \left(R_2^{11}\right)^2 F_{2;12}^{112}\right) |11\rangle \quad (40)$$

Eqs. (36) ~ (40) can be combined to yield $(\sigma_3^{(6)})^2$.

Appendix B: Reduction of Active Anyon Manipulation in Double-Braiding

We now illustrate how double-braiding topologically reduces the number of non-Abelian anyons that require active manipulation, using braidwords obtained from the $SU(2)_3$ model as concrete examples.

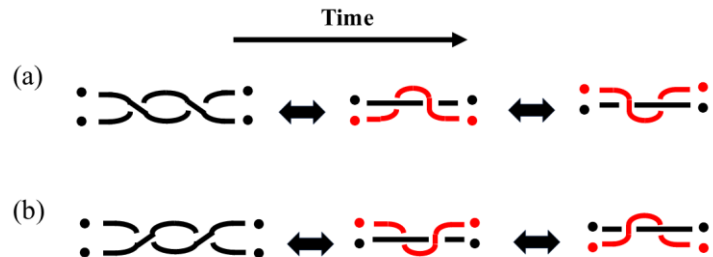


FIG. 8: The double-braiding of two anyons is topologically equivalent to one anyon making a full exchange around the other. Cases shown are for (a) clockwise and (b) counterclockwise double-braiding.

Fig. 8(a) shows that performing two consecutive clockwise braids between two anyons is topologically equivalent to winding one anyon around the other by a full circle; the counterclockwise case is shown in Fig. 8(b).

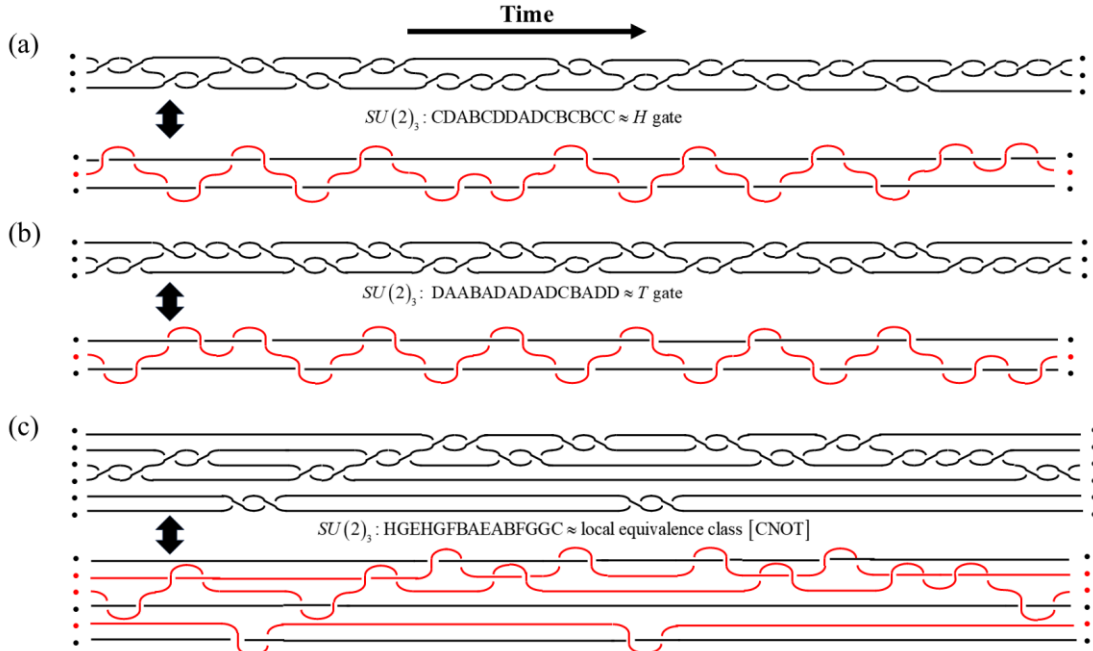


FIG. 9: Worldlines of braidwords approximating target gates. Braidwords for (a) the H gate, (b) the T gate (both up to a global phase), and (c) the local equivalence class $[CNOT]$ were found via the GA using double-braiding of $SU(2)_3$ anyons. For each panel, the upper and lower worldline depictions are topologically equivalent. The anyon to be moved in the lower depiction is highlighted in red.

By applying the local topological transformations depicted in Fig. 8, the worldlines corresponding to the DEBM-derived braidwords for the $SU(2)_3$ model (explicitly, the braidwords of H and T gates listed in Table I and the braidword of $CNOT$ in Table II) can be equivalently transformed from the configurations shown in the upper panels of Fig. 9 to those in the lower panels, which involve moving fewer anyons. Specifically, for single-qubit braiding as shown in Fig. 9 (a) and Fig. 9 (b), only the second anyon (counting from top to bottom) needs to be moved around the first and third anyons, while the others remain stationary. For two-qubit braiding, it suffices to move only the second, third, and fourth anyons; all others can be kept at rest.

References

- [1] Harrow A W and Montanaro A. Quantum computational supremacy, *Nature* 549 (2017) 203, <https://doi.org/10.1038/nature23458>
- [2] Nayak C, Simon S H, Stern A, Freedman M, and Das Sarma S. Non-Abelian anyons and topological quantum computation, *Reviews of Modern Physics* 80 (2008) 1083,

<https://doi.org/10.1103/RevModPhys.80.1083>

- [3] Kitaev A Y. Fault-tolerant quantum computation by anyons, *Annals of Physics* 303 (2003) 2, [https://doi.org/10.1016/S0003-4916\(02\)00018-0](https://doi.org/10.1016/S0003-4916(02)00018-0)
- [4] Wang D, Kong L, Fan P, Chen H, Zhu S, Liu W, Cao L, Sun Y, Du S, and Schneeloch J. Evidence for Majorana bound states in an iron-based superconductor, *Science* 362 (2018) 333, <https://doi.org/10.1126/science.aoa1797>
- [5] Kasahara Y, Ohnishi T, Mizukami Y, Tanaka O, Ma S, Sugii K, Kurita N, Tanaka H, Nasu J, and Motome Y. Majorana quantization and half-integer thermal quantum Hall effect in a Kitaev spin liquid, *Nature* 559 (2018) 227, <https://doi.org/10.1038/s41586-018-0274-0>
- [6] Witten E. Quantum field theory and the Jones polynomial, *Communications in Mathematical Physics* 121 (1989) 351, <https://doi.org/10.1007/BF01217730>
- [7] Freedman M H, Larsen M J, and Wang Z. The Two-Eigenvalue Problem and Density of Jones Representation of Braid Groups, *Communications in Mathematical Physics* 228 (2002) 177, <https://doi.org/10.1007/s002200200636>
- [8] Long J, Li Y, Zhong J, and Meng L. The construction of a universal quantum gate set for the $SU(2)^k$ ($k=5,6,7$) anyon models via genetic optimized algorithm, *Physics Letters A* 565 (2026) 131142, <https://doi.org/10.1016/j.physleta.2025.131142>
- [9] Rezayi E H and Haldane F D M. Incompressible Paired Hall State, Stripe Order, and the Composite Fermion Liquid Phase in Half-Filled Landau Levels, *Physical Review Letters* 84 (2000) 4685, <https://doi.org/10.1103/PhysRevLett.84.4685>
- [10] Zhang S-Q, Hong J-S, Xue Y, Luo X-J, Yu L-W, Liu X-J, and Liu X. Ancilla-free scheme of deterministic topological quantum gates for Majorana qubits, *Physical Review B* 109 (2024) 165302, <https://doi.org/10.1103/PhysRevB.109.165302>
- [11] Zhan Y-M, Mao G-D, Chen Y-G, Yu Y, and Luo X. Dissipationless topological quantum computation for Majorana objects in the sparse-dense mixed encoding process, *Physical Review A* 110 (2024) 022609, <https://doi.org/10.1103/PhysRevA.110.022609>
- [12] Ezawa M. Systematic construction of topological-nontopological hybrid universal quantum gates based on many-body Majorana fermion interactions, *Physical Review B* 110 (2024) 045417, <https://doi.org/10.1103/PhysRevB.110.045417>
- [13] Flensberg K, von Oppen F, and Stern A. Engineered platforms for topological superconductivity and Majorana zero modes, *Nature Reviews Materials* 6 (2021) 944, <https://doi.org/10.1038/s41578-021-00336-6>
- [14] Mandal M, Drucker N C, Siriviboon P, Nguyen T, Boonkird A, Lamichhane T N, Okabe R, Chotrattanapituk A, and Li M. Topological Superconductors from a Materials Perspective, *Chemistry of Materials* 35 (2023) 6184, <https://doi.org/10.1021/acs.chemmater.3c00713>
- [15] Fan Z and de Garis H. Braid matrices and quantum gates for Ising anyons topological quantum computation, *The European Physical Journal B* 74 (2010) 419, <https://doi.org/10.1140/epjb/e2010-00087-4>
- [16] Bonderson P, Clarke D J, Nayak C, and Shtengel K. Implementing Arbitrary Phase Gates with Ising Anyons, *Physical Review Letters* 104 (2010) 180505, <https://doi.org/10.1103/PhysRevLett.104.180505>

- [17] Iulianelli F, Kim S, Sussan J, and Lauda A D. Universal quantum computation using Ising anyons from a non-semisimple topological quantum field theory, *Nature Communications* 16 (2025) 6408, <https://doi.org/10.1038/s41467-025-61342-8>
- [18] Freedman M H, Larsen M, and Wang Z. A Modular Functor Which is Universal for Quantum Computation, *Communications in Mathematical Physics* 227 (2002) 605, <https://doi.org/10.1007/s002200200645>
- [19] Read N and Rezayi E. Beyond paired quantum Hall states: Parafermions and incompressible states in the first excited Landau level, *Physical Review B* 59 (1999) 8084, <https://doi.org/10.1103/PhysRevB.59.8084>
- [20] Hastings M B, Nayak C, and Wang Z. Metaplectic anyons, Majorana zero modes, and their computational power, *Physical Review B* 87 (2013) 165421, <https://doi.org/10.1103/PhysRevB.87.165421>
- [21] Cui S X and Wang Z. Universal quantum computation with metaplectic anyons, *Journal of Mathematical Physics* 56 (2015), <https://doi.org/10.1063/1.4914941>
- [22] Levaillant C, Bauer B, Freedman M, Wang Z, and Bonderson P. Universal gates via fusion and measurement operations on $SU(2)$ 4 anyons, *Physical Review A* 92 (2015) 012301, <https://doi.org/10.1103/PhysRevA.92.012301>
- [23] Long J, Zhong J, and Meng L. Topological quantum compilation of metaplectic anyons based on the genetic optimized algorithms, *Physical Review A* 112 (2025) 022421, <https://doi.org/10.1103/1.4914941>
- [24] Peterson M R, Wu Y-L, Cheng M, Barkeshli M, Wang Z, and Das Sarma S. Abelian and non-Abelian states in $\nu=2/3$ bilayer fractional quantum Hall systems, *Physical Review B* 92 (2015) 035103, <https://doi.org/10.1103/PhysRevB.92.035103>
- [25] Hormozi L, Zikos G, Bonesteel N E, and Simon S H. Topological quantum compiling, *Physical Review B* 75 (2007) 165310, <https://doi.org/10.1103/PhysRevB.75.165310>
- [26] Dawson C M and Nielsen M A. The Solovay-Kitaev algorithm, *Quantum Information & Computation* 6 (2006) 81, <https://dl.acm.org/doi/abs/10.5555/2011679.2011685>
- [27] McDonald R B and Katzgraber H G. Genetic braid optimization: A heuristic approach to compute quasiparticle braids, *Physical Review B* 87 (2013) 054414, <https://doi.org/10.1103/PhysRevB.87.054414>
- [28] Zhang Y-H, Zheng P-L, Zhang Y, and Deng D-L. Topological quantum compiling with reinforcement learning, *Physical Review Letters* 125 (2020) 170501, <https://doi.org/10.1103/PhysRevLett.125.170501>
- [29] Génetay Johansen E and Simula T J P Q. Fibonacci anyons versus Majorana fermions: A Monte Carlo approach to the compilation of braid circuits in $SU(2)$ k anyon models, *PRX Quantum* 2 (2021) 010334, <https://doi.org/10.1103/PRXQuantum.2.010334>
- [30] Long J, Huang X, Zhong J, and Meng L. Genetic algorithm enhanced Solovay-Kitaev algorithm for quantum compiling of Fibonacci anyons, *Physica Scripta* (2025), <https://doi.org/10.1088/1402-4896/ae1d30>
- [31] Das Sarma S, Freedman M, and Nayak C. Topological quantum computation, *Physics today* 59 (2006) 32, <https://doi.org/10.1063/1.2337825>
- [32] Burke P C, Aravanis C, Aspman J, Mareček J, and Vala J. Topological quantum

compilation of two-qubit gates, *Physical Review A* 110 (2024) 052616, <https://doi.org/10.1103/PhysRevA.110.052616>

[33] Mironov S and Morozov A. Entangling gates from cabling of knots, *The European Physical Journal C* 85 (2025) 799, <https://doi.org/10.1140/epjc/s10052-025-14492-4>

[34] Tounsi A, Belaloui N E, Louamri M M, Benslama A, and Rouabah M T. Optimized topological quantum compilation of three-qubit controlled gates in the Fibonacci anyon model: A controlled-injection approach, *Physical Review A* 110 (2024) 012603, <https://doi.org/10.1103/PhysRevA.110.012603>

[35] Xu H and Taylor J. Unified approach to topological quantum computation with anyons: From qubit encoding to Toffoli gate, *Physical Review A* 84 (2011) 012332, <https://doi.org/10.1103/PhysRevA.84.012332>

[36] Kaufmann A L and Cui S X. Universal topological quantum computing via double-braiding in SU(2) Witten–Chern–Simons theory, *Quantum Information Processing* 24 (2025) 14, <https://doi.org/10.1007/s11128-024-04633-1>

[37] Simon S H, Bonesteel N E, Freedman M H, Petrovic N, and Hormozi L. Topological Quantum Computing with Only One Mobile Quasiparticle, *Physical Review Letters* 96 (2006) 070503, <https://doi.org/10.1103/PhysRevLett.96.070503>

[38] Kazhdan D and Lusztig G. Affine Lie algebras and quantum groups, *International Mathematics Research Notices* 1991 (1991) 21, <https://doi.org/10.1155/S1073792891000041>

[39] Slingerland R A a J K. Topological qubit design and leakage, *New Journal of Physics* 13 (2011), <https://doi.org/10.1088/1367-2630/13/6/065030>

[40] Cui S X, Tian K T, Vasquez J F, Wang Z, and Wong H M. The search for leakage-free entangling Fibonacci braiding gates, *Journal of Physics A: Mathematical and Theoretical* 52 (2019) 455301, <https://doi.org/10.1088/1751-8121/ab488e>

[41] Wang Z, *Topological Quantum Computation* (American Mathematical Society, 2010), Vol. 112.

[42] Holland J H. Genetic Algorithms, *Scientific American* 267 (1992) 66, <https://doi.org/10.1038/scientificamerican0792-66>

[43] Field B and Simula T. Introduction to topological quantum computation with non-Abelian anyons, *Quantum Science and Technology* 3 (2018) 045004, <https://doi.org/10.1088/2058-9565/aacad2>

[44] Fowler A G, Stephens A M, and Groszkowski P. High-threshold universal quantum computation on the surface code, *Physical Review A* 80 (2009) 052312, <https://doi.org/10.1103/PhysRevA.80.052312>

[45] Fowler A G, Mariantoni M, Martinis J M, and Cleland A N. Surface codes: Towards practical large-scale quantum computation, *Physical Review A* 86 (2012) 032324, <https://doi.org/10.1103/PhysRevA.86.032324>

[46] Makhlin Y. Nonlocal properties of two-qubit gates and mixed states, and the optimization of quantum computations, *Quantum Information Processing* 1 (2002) 243, <https://doi.org/10.1023/A:1022144002391>

[47] Zhang J, Vala J, Sastry S, and Whaley K B. Geometric theory of nonlocal two-qubit operations, *Physical Review A* 67 (2003) 042313,

<https://doi.org/10.1103/PhysRevA.67.042313>

[48] Müller M M, Reich D M, Murphy M, Yuan H, Vala J, Whaley K, Calarco T, and Koch C. Optimizing entangling quantum gates for physical systems, *Physical Review A* 84 (2011) 042315, <https://doi.org/10.1103/PhysRevA.84.042315>